



## Characterization of the expression of the hypoxia-induced genes neuritin, TXNIP and IGFBP3 in cancer.

Sébastien Le Jan, Nolwenn Le Meur, Aurélie Cazes, Josette Philippe, Martine Le Cunff, Jean Léger, Pierre Corvol, Stéphane Germain

### ► To cite this version:

Sébastien Le Jan, Nolwenn Le Meur, Aurélie Cazes, Josette Philippe, Martine Le Cunff, et al.. Characterization of the expression of the hypoxia-induced genes neuritin, TXNIP and IGFBP3 in cancer.. FEBS Letters, 2006, 580 (14), pp.3395-400. 10.1016/j.febslet.2006.05.011 . inserm-00073189

**HAL Id: inserm-00073189**

**<https://inserm.hal.science/inserm-00073189>**

Submitted on 2 Jun 2006

**HAL** is a multi-disciplinary open access archive for the deposit and dissemination of scientific research documents, whether they are published or not. The documents may come from teaching and research institutions in France or abroad, or from public or private research centers.

L'archive ouverte pluridisciplinaire **HAL**, est destinée au dépôt et à la diffusion de documents scientifiques de niveau recherche, publiés ou non, émanant des établissements d'enseignement et de recherche français ou étrangers, des laboratoires publics ou privés.

CHARACTERIZATION OF THE EXPRESSION OF THE HYPOXIA-INDUCED GENES  
NEURITIN, TXNIP AND IGFBP3 IN CANCER

Sébastien Le Jan<sup>1,2</sup>, Nolwenn Le Meur<sup>3</sup>, Aurélie Cazes<sup>1,2</sup>, Philippe Josette<sup>1,2</sup>, Martine Le Cunff<sup>3</sup>, Jean Léger<sup>3</sup>, Pierre Corvol<sup>1,2</sup> and Stéphane Germain<sup>1,2,4</sup>

From <sup>1</sup> INSERM, Unit 36;

<sup>2</sup> Collège de France, 11 place Marcelin Berthelot, 75005 Paris, France ;

<sup>3</sup> INSERM Unit 533, Faculté de Médecine, 44000 Nantes, France ;

<sup>4</sup> Service d'Hématologie Biologique A - AP-HP - Hôpital Européen Georges Pompidou, Paris, France ;

Address correspondence to : Stéphane Germain, INSERM U36 – Collège de France, 11, place  
Marcelin Berthelot 75005 Paris – France, Tel : 33 1 44 27 1664 ; Fax : 33 1 44 27 1691

E-Mail : [stephane.germain@college-de-france.fr](mailto:stephane.germain@college-de-france.fr)

**Abstract:**

By triggering an adaptive response to hypoxia which is a common feature of tumor microenvironments, endothelial cells contribute to the onset of angiogenic responses involved in tumor growth. Therefore, identifying hypoxic markers represent a challenge for a better understanding of tumor angiogenesis and for the optimization of anti-angiogenic therapeutic strategy. Using Representational Difference Analysis combined with microarray, we here report the identification of 133 hypoxia-induced transcripts in human microendothelial cells (HMEC-1). By Northern Blot, we confirm **hypoxia-induced** expression of Insulin-like growth factor binding protein 3 (*igfbp3*), thioredoxin-interacting protein (*txnip*), neuritin (*nrn1*). Finally, by performing *in situ* hybridization on several types of human tumors, we provide evidence for *nrn1* and *txnip* as hypoxic perinecrotic markers and for *igfbp3* as a tumor endothelial marker. We propose these hypoxia-induced genes could represent relevant prognostic tools and targets for therapeutic intervention in cancers.

**Keywords:** angiogenesis, hypoxia, endothelial cells, gene expression, tumor markers

**List of abbreviations:** HMEC-1, Human MicroEndothelial Cells 1; IGFBP3, Insulin-like growth factor binding protein 3 ; TXNIP, thioredoxin-interacting protein ; NRN1, neuritin

## **1. Introduction:**

By exercising control over gene transcription, hypoxia is a common feature of several human pathologies, including cardiovascular diseases and cancer. In solid tumors, the balance between cell proliferation and oxygen supply is affected, leading to a decrease in oxygen partial pressure (pO<sub>2</sub>) [1]. Hypoxic cells trigger an adaptative molecular response to modulate expression of many genes in order to allow better perfusion and (pO<sub>2</sub>) increase in tumor tissue. Hypoxia-induced gene expression is under the control of key-transcription factors, the Hypoxia-Inducible Factors (HIFs) [2], involving posttranslational modifications of the  $\alpha$ -subunit which determine both half-life and transcriptional activity on target genes [3,4].

Angiogenesis promotes not only tumor growth, but also progression from a pre-malignant to a malignant and invasion tumor phenotype. In the tumor microenvironment, hypoxia appears to target a multiplicity of cell types which participate in tumor progression and endothelial cells are widely involved in tumor angiogenesis. In this context, targeting the tumor vasculature to « normalize » it [5] temporarily or to eradicate it completely seems to be a promising anti-cancer-therapeutic strategy [6]. To this aim, gene expression profiles of tumor cells [7] but also of endothelial cells in response to hypoxia were characterized by using microarray technologies or differential screening techniques [8-11]. However, new markers are needed for a better understanding of the hypoxia-induced angiogenesis in tumors and for the development of new diagnostic, prognostic and therapeutic tools in cancer [8]. Here, we first report a novel repertoire of hypoxia-induced transcripts (HITs) in human microendothelial cells HMEC-1 using mRNA differential screening by cDNA Representational Difference Analysis (cDNA RDA) [12] and cDNA microarray. We then described mRNA expression of HITs, particularly Neuritin (*nrn1*), Thioredoxin-interacting protein (*txnip*) and Insulin-like growth factor binding protein 3 (*igfbp3*), in various types of human tumors. Based on these observations, we therefore propose these HITs might represent relevant prognostic tools and targets for therapeutical intervention in cancers.

## **2. Material and Methods:**

### **Cell culture and tissues**

Primary cultures of HUVEC at passage 3 were cultured in EGM-2 medium (Cambrex) with 2% FBS and HMEC-1 (human dermal microvasvular endothelial cells, a gift from Thomas J. Lawley, Emory University, School of Medicine, Atlanta, GA) maintained as previously described. For hypoxic treatments, cells were grown in an atmosphere containing 2% O<sub>2</sub>, in an IG750 incubator (Jouan, France), or in the presence of 100 µmol/L of DFO for 20 hours.

All tumor tissues were obtained from the Pathological Anatomy Department of Tenon Hospital (Paris, France). Tissues were fixed in 20% formaldehyde and embedded in paraffin. Human tumors were classified according to the revised World Health Organization criteria for tumors.

### **RNA isolation and cDNA synthesis**

Total RNA was isolated from HMEC-1 and HUVEC cultured in hypoxic and normoxic conditions using the RNeasy midiprep kit from Qiagen. RNA was digested with RNase-free DNase RQ1 (Promega) for 30 minutes and 10 µg of poly(A)<sup>+</sup> RNA, prepared by performing the Oligotex mRNA kit (Qiagen) procedures twice, were used to synthesize double-stranded cDNA using oligodT priming and Superscript II (Invitrogen).

### **cDNA Representational Difference Analysis**

Representational difference analysis of cDNAs was performed as described previously [12] with several important modifications [13,14]. Subtracted RDA products were inserted into the pGEM-T cloning vector (Promega) and analyzed by sequencing. Classification of the HITS was performed according to S.O.U.R.C.E. database [15].

### **Gene expression analysis**

The cDNA microarray was constructed by combining both the HITS obtained by the cDNA RDA and the cDNA library described by Steenman *et al.* [16]. cDNA microarray construction and hybridization was performed as in Steenman *et al.* [16]. Data were pre-processed with MADSCAN [17]. To normalize intensity values the rank invariant method was used [18]. This method selects invariant gene reporters on which a nonlinear regression method (*lowess fitness*) is applied to calculate the normalization correction factor [19]. The identification of genes with statistically significant

differential expression between the two populations of cells was performed using the *limma* R package [20]. False discovery rate (FDR) correction was applied to take into account multiple testing hypotheses. Significance levels were set to  $p < 0.05$  and  $p < 0.01$ . Genes below these thresholds were considered significantly differentially expressed.

Northern Blots were performed using NorthernMax kit from Ambion. Briefly, 20µg/lane of total RNA was fractionated by 1% denaturing gel electrophoresis and transferred to nylon membranes (Hybond N<sup>+</sup> ; Amersham Biosciences). The blots were hybridized with <sup>32</sup>P-labeled cDNA probes (Random Primer DNA Labeling System ; Invitrogen) overnight at 42°C in the UltraHyb solution (Ambion). Paraffin section preparation, probe labeling by *in vitro* transcription, and *in situ* hybridization were performed as previously described [14].

### **Immunohistochemistry**

Immunostaining with a polyclonal goat anti-human IGFBP3 (1/50; R&D Systems AF675) antibody was performed by routine methods using a biotinylated secondary antibody and the ABC-peroxidase complex (Vector Laboratories) with diaminobenzidine-H<sub>2</sub>O<sub>2</sub> used as the chromogen for detection.

### **3. Results and Discussion:**

In order to identify genes whose expression is induced by hypoxia in endothelial cells, we performed a differential screening by cDNA Representational Difference Analysis between HMEC-1 cells, the first immortalized endothelial cells which retains the main characteristics of primary endothelial cells, cultured in normoxia (20% O<sub>2</sub>) or in the presence of the iron chelator desferoxamine, thus mimicking hypoxia for 20 hours. Both normoxic and hypoxic cDNA libraries are prepared and three successive rounds of hybridization/PCR amplification were performed allowing to obtain cDNAs which are overexpressed in hypoxia compared to normoxia. 1000 clones were subsequently sequenced and 300 non-redundant cDNA fragments were identified. These HITs were used for creating a cDNA microarray slide which was then hybridized with cDNAs from HMEC-1 cultured either in chemical (DFO 100 µM), gaseous (2% O<sub>2</sub>) hypoxia or normoxia for 20 hours. The data were subjected to statistical analysis allowing the identification of 131 genes overexpressed in endothelial cells (ECs) cultured under chemical hypoxia, of which 57 are also induced by gaseous hypoxia (**see supplementary material, table 1**). 77% were annotated genes and 23% left were ESTs or hypothetical proteins. Classification of RDA-induced genes according to S.O.U.R.C.E. confirmed most cellular functions are regulated by hypoxia. Indeed, consistent with previous observations, we observed the increased expression of genes which are involved in cellular metabolism, including glycolysis genes (*tpi1*, *g3pdb*, *hk2*, *eno1*, *ldha*) and glucose transporters (*glut3*). We further confirmed a large number of genes, such as *txnip*, *igfbp3* and *angptl4*, which have already been shown to be overexpressed in primary endothelial cell lines as HUVECs, HAECs and HPAECs in previous transcriptome studies using various approaches [8-11]. Interestingly, we provided evidence for new endothelial HITs such as *neuritin*, *neuroleukin*, *stk25*, *csnk1e* and *snrk*, *plectin* and *cortactin* involved in neurogenesis/neuritogenesis, signal transduction and cytoskeletal organisation respectively.

In order to further confirm hypoxia induction, we performed Northern Blot analysis on HMEC-1 and HUVEC cultured in hypoxic conditions, specifically for the pro-apoptotic gene *igfbp3*, the tumor and metastasis suppressor gene *txnip* and the firstly described hypoxia-induced gene neuritin1 (*nrn1*). **Normalization of the genes of interest to a housekeeping gene, such as glyceraldehyde-3-phosphate dehydrogenase (GAPDH), β-actin or cyclophilin could not be**

performed here since the fact that steady-state levels of these control genes cannot be assumed in endothelial cells exposed to DFO or 2% hypoxia. Therefore, the amounts of RNA loaded were normalized by hybridization with a 28S-specific probes which is known to be a constant fraction of total RNA. We observed hypoxia-induced expression of these 3 genes in both endothelial cell types, namely HMEC-1 and HUVEC, subjected to chemical hypoxia compared to normoxia, as previously shown for *angptl4* [14], used as a control here. Lowering oxygen concentration also induced expression of *igfbp3* and *nrn1* in both HMEC-1 and HUVEC while level of expression was less important than using DFO. *Txnip* mRNA was not detected in HUVEC and only very weakly in HMEC-1 cells cultured in gaseous hypoxic conditions (**figure 1**). DFO as an iron chelator used at 100μM might be more efficient than gaseous hypoxia at 2% O<sub>2</sub> on PHD and FIH inactivation and might enhance transcription via HIF-α, which could explain differences between chemical and gaseous hypoxia-induced gene expressions. HIF-prolylhydroxylases (PHD1-3) and Factor Inhibiting HIF (FIH) are enzymes belonging to 2-oxoglutarate and Fe(II) dependent dioxygenases superfamily. They are involved in HIF-α proteasome degradation and transcription suppression by hydroxylation of oxygen-dependent degradation domain (ODDD) and C-Terminal Transactivation Domain (C-TAD) respectively and have iron (Fe<sup>2+</sup>), 2-oxoglutarate and dioxygen as co-substrates [4].

Given that both tumor and vascular cells were shown to be hypoxic in tumors, we then studied the expression of these HITs in various types of human cancers with the aim to characterize new tumor and/or tumor endothelial markers. In the present study, we focused on *nrn1*, *txnip* and *igfbp3* for which no or only few data were available concerning their *in situ* mRNA expression in cancers.

Neuritin, also called CPG15, is a GPI-anchored protein which was reported to be weakly expressed in human kidney, heart, spleen, lung [21]. Neuritin is also expressed in the liver and is well correlated to the maturation of hepatocytes [22] as well as in neuronal structures associated with plasticity in the adult [21]. NRN1 has been largely involved in neuritogenesis and was shown to promote dendritic growth [23] and the development of motor neuron axon arbors [24]. In this study, we demonstrated that *nrn1* gene is expressed and induced by hypoxia in ECs. Neuritin could therefore belong to the increasing family of axon guidance which could be implicated in vessel pathfinding and



network formation as recently shown for several of these molecules [25]. **To the best of our knowledge, *nrn1* mRNA expression has never been described in human biopsies from normal or tumor tissues.** Here, by performing *in situ* hybridization experiments, we examined *nrn1* mRNA expression in different human tumors such as colon and prostate tumors, renal cell carcinoma and glioblastoma. *Nrn1* is expressed in both tumor and normal epithelial cells and weakly in endothelia of blood vessels of normal and tumoral areas in colon and prostate (data not shown). For the first time, we showed that *nrn1* mRNA is reproducibly highly expressed in a restricted number of tumor cells around perinecrotic regions of conventional RCC (**figure 2: a-c**) and glioblastoma (**figure 2: d-f**), regions in which hypoxia has been reported to up-regulate gene expression [26]. **We did not detect *nrn1* expression in peritumoral areas of these two types of tumor (data not shown).** Furthermore, NRN1 has recently been implicated in tumorigenesis by promoting changes in cell morphology, anchorage-independent growth and tumor formation [27]. In this context, the fact that hypoxic tumor cells highly express neuritin makes this molecule an attractive candidate as a **hypoxic tumor marker** and a potential target for therapeutic intervention in cancers.

Thioredoxin-interacting protein is interacting and negatively regulating thioredoxin [28] and is involved in suppression of tumor growth [29]. Furthermore, in an *in vitro* model of intravasation, overexpression of TXNIP by infecting melanoma cells with adenovirus increased transendothelial migration 3-fold versus control [30]. Until now, *txnip* mRNA was reported to be downregulated in various human tumors, including breast, stomach and lung [29] and gastrointestinal cancers [31]. For the first time, we provide evidence for *txnip* overexpression in tumor cells of hypoxic perinecrotic areas of conventional RCC (**figure 2: g-i**) and glioblastoma (**figure 2: j-l**) **compared to non-hypoxic tumor cells and peritumoral tissues.** Furthermore, hypoxia is often associated with increased metastasis and poor prognosis in cancer. Therefore, *txnip* might represent a valid candidate as prognostic marker and therapeutic target for anti-metastatic treatment.

We also studied IGFBP3 expression, which is shown to have anti-IGF-1 and IGF-1-independent pro-apoptotic activities. Many studies have provided evidence for the *in vitro* induction of *igfbp3* mRNA by hypoxia in different cell types, including ES cells [32], tumor cells [7,33] and ECs [9,11,34]. *In vivo*, a marked increase of *igfbp3* mRNA was reported in the endothelium of human



corpus luteum during early phase of luteal development which is accompanied by extensive angiogenesis [35] and specifically in tumor endothelial cells of a murine breast cancer model [36]. We here provide evidence for an *igfbp3* mRNA expression in intratumoral ECs of colon carcinoma (**figure 3: a-c**), whereas tumor and normal epithelial cells of the colon don't express *igfbp3* mRNA (**data not shown**). Concerning prostate, we showed that *igfbp3* is also very highly expressed in the ECs of adenocarcinoma (**figure 3: d-f**). We also demonstrated that *igfbp3* mRNA is specifically produced by ECs of tumor blood vessels in conventional RCC classified as pT1 in tumor, node, metastasis (TNM) system. In contrast, to draw a conclusion from results obtained in patients with pT2 and pT3 conventional RCC is more difficult. Indeed, *igfbp3* mRNA is produced only by tumor cells in some patients whereas expressed by both tumor cells and intratumor ECs in some other patients (data not shown). Finally, *igfbp3* mRNA expression was investigated in chromophobe RCC. Accordingly, a very high level of *igfbp3* mRNA was observed only in ECs of tumor vessels, but not in tumor cells, of all patients with chromophobe RCC (**figure 3 : j-l**). Interestingly, *igfbp3* mRNA was not detected in peritumoral kidney of any renal tumor (**data not shown**). We further characterized IGFBP3 protein expression in these tumors by immunohistochemistry. IGFBP3 was detected in ECs of tumor vessels, but neither in tumor cells nor in tubular cells of peritumoral region, within clear-cell and chromophobe RCC (**figure 4: a and b** respectively). **These results are in accordance with previous *in vitro* study showing a very weak expression in primary proximal tubular cells and primary renal cell carcinoma [37]**. IGFBP3 is also expressed in peritumoral ECs of these tumors and in some tumor cells of chromophobe RCC. We further demonstrated a similar pattern of IGFBP3 staining in blood vessels of colon and prostate tumors (**figure 4 : c and d** respectively), with a high expression level in both tumor endothelium as well as in peritumoral ECs close to the tumor. We therefore characterize *igfbp3* gene as an endothelial marker in various human tumors. Recently, it was shown that IGFBP3 reverses proliferation and prevents the survival induced by VEGF in HUVEC [38] and that downregulation of endothelial *igfbp3* mRNA by Runx1 transcription factor promoted angiogenesis in the matrigel assay [39]. However, IGFBP3 functions in tumor-associated angiogenesis are not understood yet and have to be examined thoroughly in order to evaluate IGFBP3 suitability as a valid therapeutic target. **The present study compared *nrn1*, *txnip* and *igfbp3* mRNAs expression in**

**tumor and peritumoral area. Data concerning the expression of these genes in human biopsies from normal organs (kidney, colon, prostate) are lacking in the literature. Therefore, more detailed gene expression analyses have to be performed on normal tissues to fully consider *nrn1*, *txnip* and *igfbp3* as proper tumor markers.**

Altogether, this work provided evidence for a new set of hypoxia-induced genes in ECs *in vitro*. Overexpression of some of these genes was further observed in different cell types subjected to *in vivo* pathological hypoxia, particularly in tumor cells surrounding necrotic regions or tumor endothelial cells. In this context, we propose these genes, *txnip*, *nrn1* and *igfbp3* as hypoxic markers and potential makers in tumor angiogenesis, might become prognostic tools and potential anti-cancerous therapeutic targets.

#### **4. Acknowledgements**

We thank Dr. Mathilde Sibony (Pathological Anatomy Department of Tenon Hospital, Paris, France) for providing all tumor tissues. SLJ is a recipient of both Ministère de la Recherche and Fondation pour la Recherche Médicale fellowships. AC is a recipient of an INSERM fellowship. SG is supported by grants from la Fondation de France and Canceropole-PACA ACI 2004 and belongs to the European Vascular Genomics Network (<http://www.evgn.org>) a Network of Excellence supported by the European Community's sixth Framework Programme for Research Priority 1 "Life sciences, genomics and biotechnology for health" (Contract N° LSHM-CT-2003-503254).

## **5. References:**

- [1] Helmlinger, G., Yuan, F., Dellian, M. and Jain, R.K. (1997). Interstitial pH and pO<sub>2</sub> gradients in solid tumors in vivo: high-resolution measurements reveal a lack of correlation. *Nat Med.* 3, 177-82.
- [2] Semenza, G.L. (1998). Hypoxia-inducible factor 1: master regulator of O<sub>2</sub> homeostasis. *Curr Opin Genet Dev.* 8, 588-94.
- [3] Brahimi-Horn, C., Mazure, N. and Pouyssegur, J. (2005). Signalling via the hypoxia-inducible factor-1alpha requires multiple posttranslational modifications. *Cell Signal.* 17, 1-9.
- [4] Masson, N. and Ratcliffe, P.J. (2003). HIF prolyl and asparaginyl hydroxylases in the biological response to intracellular O<sub>2</sub> levels. *J Cell Sci.* 116, 3041-9.
- [5] Jain, R.K. (2005). Normalization of tumor vasculature: an emerging concept in antiangiogenic therapy. *Science.* 307, 58-62.
- [6] Folkman, J. (1972). Anti-angiogenesis: new concept for therapy of solid tumors. *Ann Surg.* 175, 409-16.
- [7] Lal, A., Peters, H., St Croix, B., Haroon, Z.A., Dewhirst, M.W., Strausberg, R.L., Kaanders, J.H., van der Kogel, A.J. and Riggins, G.J. (2001). Transcriptional response to hypoxia in human tumors. *J Natl Cancer Inst.* 93, 1337-43.
- [8] St Croix, B., Rago, C., Velculescu, V., Traverso, G., Romans, K.E., Montgomery, E., Lal, A., Riggins, G.J., Lengauer, C., Vogelstein, B. and Kinzler, K.W. (2000). Genes expressed in human tumor endothelium. *Science.* 289, 1197-202.
- [9] Scheurer, S.B., Rybak, J.N., Rosli, C., Neri, D. and Elia, G. (2004). Modulation of gene expression by hypoxia in human umbilical cord vein endothelial cells: A transcriptomic and proteomic study. *Proteomics.* 4, 1737-60.
- [10] Ning, W., Chu, T.J., Li, C.J., Choi, A.M. and Peters, D.G. (2004). Genome-wide analysis of the endothelial transcriptome under short-term chronic hypoxia. *Physiol Genomics.* 18, 70-8.
- [11] Manalo, D.J., Rowan, A., Lavoie, T., Natarajan, L., Kelly, B.D., Ye, S.Q., Garcia, J.G. and Semenza, G.L. (2005). Transcriptional regulation of vascular endothelial cell responses to hypoxia by HIF-1. *Blood.* 105, 659-69.

- [12] Hubank, M. and Schatz, D.G. (1999). cDNA representational difference analysis: a sensitive and flexible method for identification of differentially expressed genes. *Methods Enzymol.* 303, 325-49.
- [13] Pastorian, K., Hawel, L., 3rd and Byus, C.V. (2000). Optimization of cDNA representational difference analysis for the identification of differentially expressed mRNAs. *Anal Biochem.* 283, 89-98.
- [14] Le Jan, S., Amy, C., Cazes, A., Monnot, C., Lamande, N., Favier, J., Philippe, J., Sibony, M., Gasc, J.M., Corvol, P. and Germain, S. (2003). Angiopoietin-like 4 is a proangiogenic factor produced during ischemia and in conventional renal cell carcinoma. *Am J Pathol.* 162, 1521-8.
- [15] Diehn, M., Sherlock, G., Binkley, G., Jin, H., Matese, J.C., Hernandez-Boussard, T., Rees, C.A., Cherry, J.M., Botstein, D., Brown, P.O. and Alizadeh, A.A. (2003). SOURCE: a unified genomic resource of functional annotations, ontologies, and gene expression data. *Nucleic Acids Res.* 31, 219-23.
- [16] Steenman, M., Lamirault, G., Le Meur, N., Le Cunff, M., Escande, D. and Leger, J.J. (2005). Distinct molecular portraits of human failing hearts identified by dedicated cDNA microarrays. *Eur J Heart Fail.* 7, 157-65.
- [17] Le Meur, N., Lamirault, G., Bihouee, A., Steenman, M., Bedrine-Ferran, H., Teusan, R., Ramstein, G. and Leger, J.J. (2004). A dynamic, web-accessible resource to process raw microarray scan data into consolidated gene expression values: importance of replication. *Nucleic Acids Res.* 32, 5349-58.
- [18] Tseng, G.C., Oh, M.K., Rohlin, L., Liao, J.C. and Wong, W.H. (2001). Issues in cDNA microarray analysis: quality filtering, channel normalization, models of variations and assessment of gene effects. *Nucleic Acids Res.* 29, 2549-57.
- [19] Yang, Y.H., Dudoit, S., Luu, P., Lin, D.M., Peng, V., Ngai, J. and Speed, T.P. (2002). Normalization for cDNA microarray data: a robust composite method addressing single and multiple slide systematic variation. *Nucleic Acids Res.* 30, e15.
- [20] Smyth, G.K. (2004) in: *Statistical Applications in Genetics and Molecular Biology*, Vol. 3: No. 1, Article 3.

- [21] Naeve, G.S., Ramakrishnan, M., Kramer, R., Hevroni, D., Citri, Y. and Theill, L.E. (1997). Neuritin: a gene induced by neural activity and neurotrophins that promotes neuritogenesis. *Proc Natl Acad Sci U S A*. 94, 2648-53.
- [22] Kojima, N., Shiojiri, N., Sakai, Y. and Miyajima, A. (2005). Expression of neuritin during liver maturation and regeneration. *FEBS Lett*. 579, 4562-6.
- [23] Nedivi, E., Wu, G.Y. and Cline, H.T. (1998). Promotion of dendritic growth by CPG15, an activity-induced signaling molecule. *Science*. 281, 1863-6.
- [24] Javaherian, A. and Cline, H.T. (2005). Coordinated motor neuron axon growth and neuromuscular synaptogenesis are promoted by CPG15 in vivo. *Neuron*. 45, 505-12.
- [25] Eichmann, A., Le Noble, F., Autiero, M. and Carmeliet, P. (2005). Guidance of vascular and neural network formation. *Curr Opin Neurobiol*. 15, 108-15.
- [26] Onita, T., Ji, P.G., Xuan, J.W., Sakai, H., Kanetake, H., Maxwell, P.H., Fong, G.H., Gabril, M.Y., Moussa, M. and Chin, J.L. (2002). Hypoxia-induced, perinecrotic expression of endothelial Per-ARNT-Sim domain protein-1/hypoxia-inducible factor-2alpha correlates with tumor progression, vascularization, and focal macrophage infiltration in bladder cancer. *Clin Cancer Res*. 8, 471-80.
- [27] Raggio, C., Ruhl, R., McAllister, S., Koon, H., Dezube, B.J., Fruh, K. and Moses, A.V. (2005). Novel cellular genes essential for transformation of endothelial cells by Kaposi's sarcoma-associated herpesvirus. *Cancer Res*. 65, 5084-95.
- [28] Nishiyama, A., Matsui, M., Iwata, S., Hirota, K., Masutani, H., Nakamura, H., Takagi, Y., Sono, H., Gon, Y. and Yodoi, J. (1999). Identification of thioredoxin-binding protein-2/vitamin D(3) up-regulated protein 1 as a negative regulator of thioredoxin function and expression. *J Biol Chem*. 274, 21645-50.
- [29] Han, S.H., Jeon, J.H., Ju, H.R., Jung, U., Kim, K.Y., Yoo, H.S., Lee, Y.H., Song, K.S., Hwang, H.M., Na, Y.S., Yang, Y., Lee, K.N. and Choi, I. (2003). VDUP1 upregulated by TGF-beta1 and 1,25-dihydroxyvitamin D3 inhibits tumor cell growth by blocking cell-cycle progression. *Oncogene*. 22, 4035-46.

- [30] Cheng, G.C., Schulze, P.C., Lee, R.T., Sylvan, J., Zetter, B.R. and Huang, H. (2004). Oxidative stress and thioredoxin-interacting protein promote intravasation of melanoma cells. *Exp Cell Res.* 300, 297-307.
- [31] Ikarashi, M., Takahashi, Y., Ishii, Y., Nagata, T., Asai, S. and Ishikawa, K. (2002). Vitamin D3 up-regulated protein 1 (VDUP1) expression in gastrointestinal cancer and its relation to stage of disease. *Anticancer Res.* 22, 4045-8.
- [32] Feldser, D., Agani, F., Iyer, N.V., Pak, B., Ferreira, G. and Semenza, G.L. (1999). Reciprocal positive regulation of hypoxia-inducible factor 1alpha and insulin-like growth factor 2. *Cancer Res.* 59, 3915-8.
- [33] Koong, A.C., Denko, N.C., Hudson, K.M., Schindler, C., Swiersz, L., Koch, C., Evans, S., Ibrahim, H., Le, Q.T., Terris, D.J. and Giaccia, A.J. (2000). Candidate genes for the hypoxic tumor phenotype. *Cancer Res.* 60, 883-7.
- [34] Tucci, M., Nygard, K., Tanswell, B.V., Farber, H.W., Hill, D.J. and Han, V.K. (1998). Modulation of insulin-like growth factor (IGF) and IGF binding protein biosynthesis by hypoxia in cultured vascular endothelial cells. *J Endocrinol.* 157, 13-24.
- [35] Fraser, H.M., Lunn, S.F., Kim, H. and Erickson, G.F. (1998). Insulin-like growth factor binding protein-3 mRNA expression in endothelial cells of the primate corpus luteum. *Hum Reprod.* 13, 2180-5.
- [36] Schmid, M.C., Bisoffi, M., Wetterwald, A., Gautschi, E., Thalmann, G.N., Mitola, S., Bussolino, F. and Cecchini, M.G. (2003). Insulin-like growth factor binding protein-3 is overexpressed in endothelial cells of mouse breast tumor vessels. *Int J Cancer.* 103, 577-86.
- [37] Cheung, C.W., Vesey, D.A., Nicol, D.L. and Jonhson, D.W. (2004). The roles of IGF-I and IGFBP-3 in the regulation of proximal tubule, and renal cell carcinoma cell proliferation. *Kidney int.* 65, 1272-79.
- [38] Franklin, S.L., Ferry, R.J., Jr. and Cohen, P. (2003). Rapid insulin-like growth factor (IGF)-independent effects of IGF binding protein-3 on endothelial cell survival. *J Clin Endocrinol Metab.* 88, 900-7.

- [39] Iwatsuki, K., Tanaka, K., Kaneko, T., Kazama, R., Okamoto, S., Nakayama, Y., Ito, Y., Satake, M., Takahashi, S.I., Miyajima, A., Watanabe, T. and Hara, T. (2005). Runx1 promotes angiogenesis by downregulation of insulin-like growth factor-binding protein-3. *Oncogene*. 24, 1129-37.



## **6. Figure legends:**

**Figure 1 :** Confirmation of cDNA microarray by Northern Blot analysis. Total RNA from HMEC-1 and HUVEC cultured in normoxia or hypoxia (100μM DFO or 2% O<sub>2</sub>) were fractionated on a formaldehyde agarose gel, transferred to a nylon membrane and probed with <sup>32</sup>P-labeled probes for *igfbp3*, *nrn1*, *txnip* and *angptl4* mRNAs.

**Figure 2 :** *Nrn1* and *Txnip*, markers of perinecrotic regions in conventional RCC and glioblastoma. Bright field (**left** and **right**) and dark field (**middle**) views of *nrn1* and *txnip* mRNA production in perinecrotic region of conventional RCC (**a-c** and **g-i** respectively) and glioblastoma (**d-f** and **j-l** respectively). N, necrosis area . Scale bars, 50μm.

**Figure 3 :** *Igfbp3* mRNA, a tumor endothelial marker in various types of human tumors. HES (**left**), dark field (**middle**) and bright field (**right**) views of *igfbp3* mRNA expression in endothelial cells of colon adenocarcinoma (**a-c**), prostate adenocarcinoma (**d-f**), conventional RCC (**g-i**) and chromophobe RCC (**j-l**). Scale bars, 50μm.

**Figure 4 :** Characterization of IGFBP3 protein expression in human tumors. Immunostaining for IGFBP3 protein in conventional (**a**) and chromophobe (**b**) RCC, in colon and prostate adenocarcinoma (**c** and **d** respectively). Scale bars, 50μm.

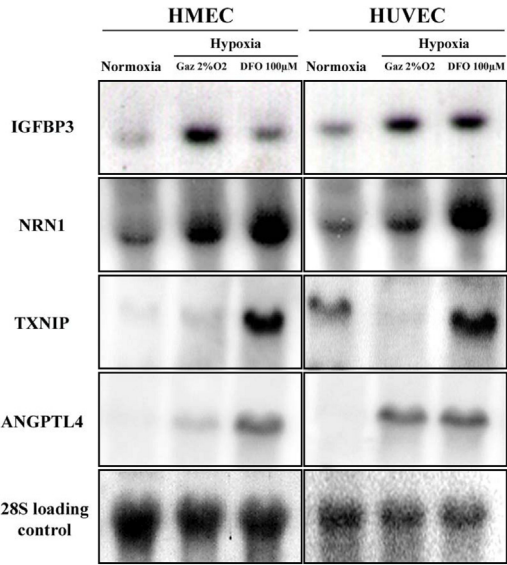
# Supplementary data : table 1

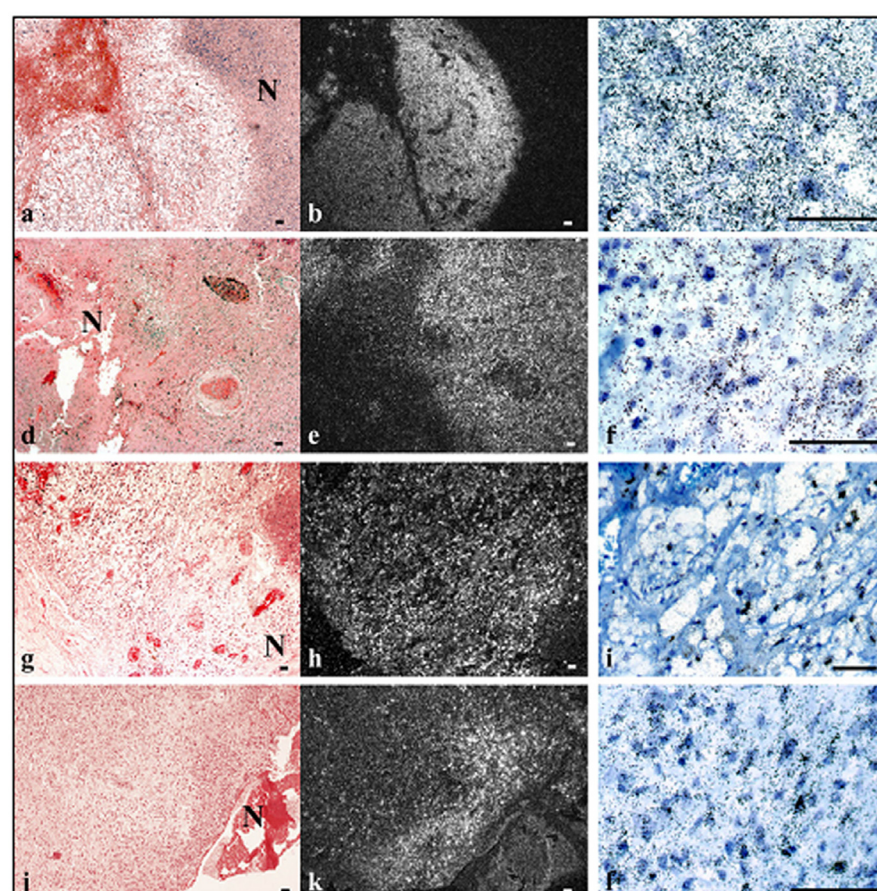
**Table 1:** Chemically and gaseous hypoxia-induced genes in HMEC-1. Hypoxia-induced genes identified by cDNA RDA were used to create a dedicated cDNA microarray. This cDNA microarray was then hybridized with cDNA from HMEC-1 cultured in normoxia or hypoxia (DFO or 2% O<sub>2</sub>). Statistical analysis was performed and difference of gene expression between DFO and gaz was analysed ( - : non significantly different; \* : p<0,05; \*\* : p<0,01).

Accession number	Symbol	Full Name	DFO Fold change	GAZ Fold change	Difference between DFO and GAZ
<b>Angiogenesis</b>					
202636	ANGPTL4	angiopoietin-like 4	2,68	1,89	**
23021	unknown	Human tissue plasminogen activator (PLAT) gene, complete cds	1,73	1,26	*
28593	JAG1	jagged 1 (Alagille syndrome)	1,35	-	-
14083	SERPINE1	serine (or cysteine) proteinase inhibitor, clade E (nexin, plasminogen activator inhibitor type 1), member 1	1,28	-	-
25195	ROBO4	roundabout homolog 4, magic roundabout (Drosophila)	1,16	-	-
<b>Cell adhesion/ Cell migration</b>					
34150	LOX	lysyl oxidase	2,48	1,78	*
20441	P4HA2	procollagen-proline, 2-oxoglutarate 4-dioxygenase (proline 4-hydroxylase), alpha polypeptide II	1,93	-	-
223207	CHSY1	carbohydrate (chondroitin) synthase 1	1,78	1,62	-
10905	FN1	fibronectin 1	1,74	1,34	**
24131	PTPRB	protein tyrosine phosphatase, receptor type, B	1,6	1,3	*
2031617	THBS1	thrombospondin 1	1,53	1,42	-
26729	COL5A1	collagen, type V, alpha 1	1,4	-	-
25593	HUMTIMP2	Human metalloproteinase-2 inhibitor (TIMP-2) mRNA, complete cds	1,39	-	-
20815	PTPRF	protein tyrosine phosphatase, receptor type, F	1,35	-	-
2002318	LOXL2	lysyl oxidase-like 2	1,3	-	-
20341	unknown	cDNA encoding human pro-cathepsin B.	1,15	-	-
<b>Cell growth/ Maintenance/ Apoptosis:</b>					
204162	NDRG1	N-myc downstream regulated gene 1	2,77	1,21	**
2038124	IGFBP3	insulin-like growth factor binding protein 3	1,77	1,52	-
209465	TNFAIP3	tumor necrosis factor, alpha-induced protein 3	1,67	1,21	**
26104	DAPK1	death-associated protein kinase 1	1,64	1,53	-
29639	EXT1	exostoses (multiple) 1	1,60	1,41	-
2016794	HD	huntingtin (Huntington disease)	1,53	-	-
212783	PDGFB	platelet-derived growth factor beta polypeptide (simian sarcoma viral (v-sis) oncogene homolog)	1,53	1,42	-
23946	RBM5	RNA binding motif protein 5	1,35	-	-
2097519	unknown	Homo sapiens podocalyxin-like protein mRNA, complete cds	1,20	-	-
21635	unknown	Human OS-9 precursor mRNA, complete cds	1,16	-	-
<b>Cell Structure</b>					
208343	CTTN	cortactin	2,58	1,58	**
2080044	PLEC1	plectin 1, intermediate filament binding protein 500kDa	2,39	1,6	*
209139	unknown	Homo sapiens myosin mRNA, partial cds.	1,47	1,21	*
2062992	SPAG4	sperm associated antigen 4	1,40	-	-
2002476	MYL4	myosin, light polypeptide 4, alkali; atrial, embryonic	1,36	-	-
295661	C16orf5	Homo sapiens transmembrane protein I1 (I1) mRNA, complete cds	1,25	-	-
204571	MAP4	microtubule-associated protein 4	1,23	-	-
206803	SPTBN1	spectrin, beta, non-erythrocytic 1	1,21	-	-
<b>Development</b>					
2094352	unknown	Human manic fringe precursor mRNA, complete cds	1,68	-	-
<b>Metabolism (lipid, carbohydrates, glycolysis ...)</b>					
2005566	LDHA	lactate dehydrogenase A	2,91	1,84	**
201829	MGAT1	mannosyl (alpha-1,3-)-glycoprotein beta-1,2-N-acetylglucosaminyltransferase	2,53	1,88	**
2018197	unknown	Human ATP:citrate lyase mRNA, complete cds	2,41	1,83	*
204328	ENO1	enolase 1, (alpha)	2,1	1,2	**
2079775	unknown	Homo sapiens NNP-1/Nop52 (NNP-1) mRNA, complete cds	1,99	1,25	**
207851	HUMG3PDB	Human glyceraldehyde-3-phosphate dehydrogenase mRNA, complete cds	1,74	-	-
2009885	TPI1	triosephosphate isomerase 1	1,74	1,22	**
202349	ENO2	enolase 2 (gamma, neuronal)	1,71	1,32	**
209735	PFKFB3	6-phosphofructo-2-kinase/fructose-2,6-biphosphatase 3	1,68	1,22	**
203849	VLDLR	very low density lipoprotein receptor	1,57	-	-
206376	unknown	H.sapiens HK2 mRNA for hexokinase II.	1,43	-	-
2000961	PTGIS	prostaglandin I2 (prostacyclin) synthase	1,41	1,2	**
204098	HDLBP	high density lipoprotein binding protein (vigilin)	1,33	-	-
207638	ASL	argininosuccinate lyase	1,3	1,16	-
<b>Neurogenesis/ Neuritogenesis</b>					
2036631	NRN1	neuritin 1	1,73	1,52	-
203515	HUMNLK	Human neuroleukin mRNA, complete cds	1,44	-	-
200976	DPYSL4	dihydropyrimidinase-like 4	1,43	-	-
<b>Protein catabolism</b>					
202389	PRSS15	protease, serine, 15	1,27	-	-
2054185	PSMA7	proteasome (prosome, macropain) subunit, alpha type, 7	1,21	-	-
2061542	CYLD	cylindromatosis (turban tumor syndrome)	1,18	-	-
<b>Protein Folding/ Stress-induced protein</b>					
203591	TXNIP	thioredoxin interacting protein	1,85	1,31	**
206719	unknown	cDNA encoding human protein disulfide isomerase.	1,72	-	-
20003299	TRA1	tumor rejection antigen (gp96) 1	1,49	-	-
203174	SERPINH1	serine (or cysteine) proteinase inhibitor, clade H (heat shock protein 47), member 1, (collagen binding protein 1)	1,30	-	-
205785	HYOU1	hypoxia up-regulated 1 = ORP150	1,27	-	-

Session number	Symbol	Full Name	DFO Fold change	GAZ Fold change	Difference between DFO and GAZ
<b>Signal transduction</b>					
6950	ADORA2A	adenosine A2a receptor	3,71	2,62	*
3780	STK25	serine/threonine kinase 25 (STE20 homolog, yeast)	2,17	1,39	**
051522	CMKOR1	chemokine orphan receptor 1	1,40	-	-
20704	PPFIA4	protein tyrosine phosphatase, receptor type, f polypeptide (PTPRF), interacting protein (liprin), alpha 4	1,38	1,19	-
2390	TRIO	triple functional domain (PTPRF interacting)	1,38	-	-
06490	CSNK1E	casein kinase 1, epsilon	1,38	-	-
2794	NR2F6	nuclear receptor subfamily 2, group F, member 6	1,35	-	-
240696	WSB1	WD repeat and SOCS box-containing 1	1,27	1,53	-
03476	AKAP12	A kinase (PRKA) anchor protein (gravin) 12	1,21	-	-
26945	TRIB3	tribbles homolog 3 (Drosophila)	1,14	-	-
26044	SNRK	SNF-1 related kinase	1,14	-	-
67784	unknown	Human orphan G protein-coupled receptor (RDC1) mRNA, partial cds	-	1,35	-
<b>Transport (glucose, protein, ion ...)</b>					
018359	POM121	POM121 membrane glycoprotein (rat)	3,63	2,48	**
20681	SLC2A3	solute carrier family 2 (facilitated glucose transporter), member 3	2,35	1,62	*
9353	GDI1	GDP dissociation inhibitor 1	2,14	1,61	*
274889	unknown	Homo sapiens glucose transporter 3 gene, exons 1 to 6.	1,79	1,4	-
036096	PTTG1P	pituitary tumor-transforming 1 interacting protein	1,71	-	-
110362	unknown	Human GP36b glycoprotein mRNA, complete cds	1,6	-	-
23115	ATP2A2	ATPase, Ca <sup>2+</sup> ; transporting, cardiac muscle, slow twitch 2	1,29	-	-
55652	KCMF1	potassium channel modulatory factor 1	1,19	-	-
11021	KCNQ2	potassium voltage-gated channel, subfamily G, member 2	1,18	1,21	-
1518	AQP1	aquaporin 1 (channel-forming integral protein, 28kDa)	1,17	-	-
8956	SLC6A6	solute carrier family 6 (neurotransmitter transporter, taurine), member 6	1,16	-	-
<b>Translation/ Protein biosynthesis</b>					
39400	unknown	Homo sapiens NOF1 mRNA, complete cds	1,40	-	-
64622	GOLGIN-67	golgin-67	1,38	1,31	-
9997	EEF2	eukaryotic translation elongation factor 2	1,20	-	-
131501	unknown	Human fragile X mental retardation syndrome related protein (FXR2) mRNA, complete cds	1,15	-	-
68990	GTPBP2	GTP binding protein 2	1,15	-	-
37735	RPL14	ribosomal protein L14	-	1,17	-
<b>Other functions or unknown functions</b>					
79775	unknown	Homo sapiens NNP-1/Nop52 (NNP-1) mRNA, complete cds	1,99	1,25	**
59047	unknown	Rattus norvegicus SPANK-2 mRNA, partial cds	1,54	-	-
02602	UREB1	upstream regulatory element binding protein 1	1,52	1,31	-
70657	GSTK1	glutathione S-transferase kappa 1	1,48	-	-
042302	unknown	Homo sapiens similar to Gene 33/Mig-6 (H. sapiens) (LOC148460).mRNA.	1,47	1,21	*
7324	unknown	H.sapiens mRNA for adipophilin	1,35	-	-
23521	FER1L4	fer-1-like 4 (C. elegans)	1,35	1,45	-
051925	LBH	likely ortholog of mouse limb-bud and heart gene	1,32	-	-
240786	GSTT2	glutathione S-transferase theta 2	1,30	-	-
7078	PUM2	pumilio homolog 2 (Drosophila)	1,28	-	-
2209	HSMN1	Homo sapiens mRNA for MN1 protein	1,25	-	-
220718	CLSTN1	calsynenin 1	1,22	-	-
28965	OIP106	OGT(O-Glc-nac transferase)-interacting protein 106 KDa	1,13	-	-
<b>ESTs or Hypothetical proteins: 23,3%</b>					
747444	unknown	602704739F1 NIH_MGC_15 Homo sapiens cDNA clone IMAGE:4858161 5',mRNA sequence.	5,03	3,63	*
01776	C20orf20	Homo sapiens cDNA FLJ10914 fis, clone OVARC1000212	3,43	1,89	**
800927	unknown	Homo sapiens mRNA; cDNA DKFZp586N0721 (from clone DKFZp586N0721)	3,25	2,53	-
17505	unknown	Homo sapiens mRNA; cDNA DKFZp434E1835 (from clone DKFZp434E1835).	2,81	1,89	**
07540	LOC144097	hypothetical protein BC007540	2,17	2,07	-
801483	unknown	Homo sapiens mRNA; cDNA DKFZp434E0121 (from clone DKFZp434E0121)	2,11	1,77	-
00885	unknown	Homo sapiens cDNA FLJ10023 fis, clone HEMBA1000608, moderately similar to HYPOTHETICAL PROTEIN KIAA0411.	2,03	1,41	*
356598	unknown	EST368653 MAGE resequences, MAGD Homo sapiens cDNA, mRNA sequence.	1,91	-	-
34711	unknown	Homo sapiens C1ORF12 mRNA, 3' untranslated region, partial sequence.	1,83	1,30	**
21598	unknown	Homo sapiens cDNA FLJ11536 fis, clone HEMBA1002712.	1,64	1,55	-
011196	KIAA0676	KIAA0676 protein	1,55	1,41	-
33023	FLJ10201	hypothetical protein FLJ10201	1,49	-	-
17505	unknown	Homo sapiens mRNA; cDNA DKFZp434E1835 (from clone DKFZp434E1835)	1,47	-	-
18774	unknown	DKFZp761B0811_r1 761 (synonym: hamy2) Homo sapiens cDNA clone DKFZp761B0811 5', mRNA sequence.	1,46	1,39	-
07128	unknown	Homo sapiens clone 23870 mRNA sequence.	1,44	1,27	-
34417	unknown	Human DNA sequence from clone CTA-215D11 on chromosome 1p36.12-36.33, complete sequence	1,44	-	-
02365	KIAA0367	KIAA0367	1,43	-	-
20721	FAM13A1	Homo sapiens mRNA for KIAA0914 protein, partial cds	1,40	1,20	*
355980	unknown	EST368050 MAGE resequences, MAGD Homo sapiens cDNA, mRNA sequence.	1,33	1,18	*
86150	unknown	Homo sapiens full length insert cDNA clone ZB44E06.	1,30	-	-
92656	unknown	Homo sapiens BAC clone RP11-455G16 from 4, complete sequence.	1,26	1,17	-
80172	FLJ21919	hypothetical protein FLJ21919	1,24	-	-
26024	FLJ10307	hypothetical protein FLJ10307	1,23	-	-
48871	unknown	DKFZp4341018_r1 434 (synonym: htes3) Homo sapiens cDNA clone DKFZp4341018, mRNA sequence.	1,20	-	-
375061	unknown	602598169F1 NIH_MGC_87 Homo sapiens cDNA clone IMAGE:4706800 5',mRNA sequence.	1,20	-	-
385745	unknown	602637842F1 NIH_MGC_48 Homo sapiens cDNA clone IMAGE:4765403 5',mRNA sequence.	1,18	-	-
28534	unknown	human STS SHGC-31555, sequence tagged site.	1,18	-	-
26087	C9orf25	Homo sapiens cDNA: FLJ22434 fis, clone HRC09178, highly similar to AF131828 Homo sapiens clone 25012 mRNA sequence	1,17	-	-
61555	unknown	Homo sapiens HSPC070 mRNA, complete cds.	1,16	-	-
397805	unknown	RC1-NN0063-100500-022-c06 NN0063 Homo sapiens cDNA, mRNA sequence.	1,16	-	-
362770	unknown	EST374843 MAGE resequences, MAGG Homo sapiens cDNA, mRNA sequence.	1,15	-	-

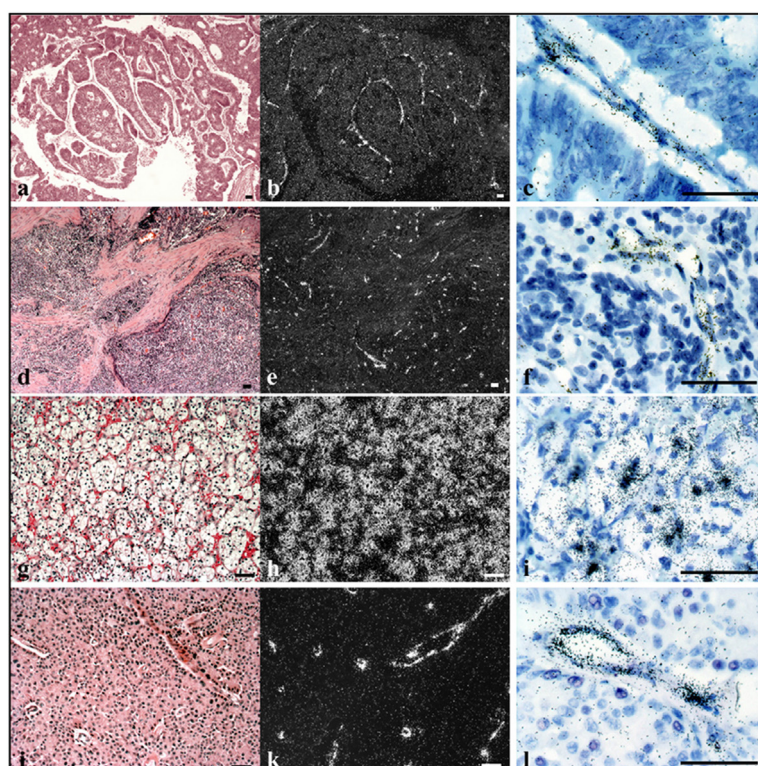
**LE JAN; FIGURE 1**



**LE JAN; FIGURE 2**



**LE JAN; FIGURE 3**



**LE JAN; FIGURE 4**

